Diversity of Parengyodontium spp. strains isolated from the cultural heritage environment: Phylogenetic diversity, phenotypical diversity, and occurrence

Johann Leplat, Alexandre François, Faisl Bousta

Diversity of *Parengyodontium* spp. strains isolated from the cultural heritage environment: phylogenetic diversity, phenotypical diversity and occurrence.

Johann Leplat[a,b*], Alexandre François[a,b], Faisl Bousta[a,b]

[a]*Laboratoire de Recherche des Monuments Historiques (LRMH), Ministère de la Culture, 29 rue de Paris, 77420 Champs-sur-Marne, France*

[b]*Sorbonne Universités, Centre de Recherche sur la Conservation (CRC, USR 3224), Museum national d'Histoire naturelle, Ministère de la Culture, CNRS; CP21, 36 rue Geoffroy-Saint-Hilaire, 75005 Paris, France*

[*]*corresponding author e-mail: johann.leplat@culture.gouv.fr*

Diversity of *Parengyodontium* spp. strains isolated from the cultural heritage environment: phylogenetic diversity, phenotypical diversity and occurrence.

ABSTRACT

Parengyodontium album is fungal species that frequently occurs in the cultural heritage environment. Although three subclades were initially described in the species, no study has sought to determine the occurrence of each subclade in the cultural heritage context. These subclades are easily distinguishable phylogenetically, but their morphological identification is more difficult. Eighteen strains isolated from different cultural sites and initially identified as *P. album* were studied phylogenetically, morphologically and in terms of their susceptibility to econazole nitrate 0.2 %, an antifungal product used as preservation treatment in cultural heritage domain. The phylogenetic study revealed that all studied strains belonged to *P. album* subclade 1 or *P. torokii* (*P. album* subclade 3), while none belonged to *P. album* subclade 2. The morphological study revealed the best characteristics to differentiate the three subclades/species, namely the ability of the strains to grow at 32 °C and 35 °C on PDA medium, and the shape of conidia. Finally, the strains displayed variable susceptibilities to econazole nitrate, with no apparent link to any particular subclade/species.

KEY WORDS

Morphology; *Parengyodontium album*; *Parengyodontium torokii*; Phylogeny; Population study; Susceptibility to antifungal products

INTRODUCTION

The genus *Parengyodontium* was added to the Cordycipitaceae family by Tsang et al. (2016) to accommodate the single species *Parengydontium album* (Limber) C.C. Tsang, J.F.W. Chan, W.M. Pong, J.H.K. Chen, A.H.Y. Ngan, M. Cheung, C.K.C. Lai, D.N.C. Tsang, S.K.P. Lau & P.C.Y. Woo, which formerly belonged to the genus *Engyodontium* for the description of the genus (De Hoog 1978). *Parengyodontium album*, which is characterized by conidiogenous cells bearing zigzag-shaped terminal regions, was different from other species in the genus *Engyodontium* in term of its phylogenetic and chemotaxonomic features. Today, the genus *Parengyodontium* is composed of only three species: *P. album*, *P. americanum* M.M. Teixeira, Wiederh. & B.M. Barker (Teixeira et al. 2020), and *P. torokii* N.K. Singh & K. Venkateswaran, which was described very recently by Parker et al. (2022).

Tsang et al. (2016) identified three subclades among *P. album* species, which were difficult to differentiate using solely phenotypical features. These authors noticed that the strains belonging to subclade 2 were the only ones able to grow at temperatures over 31 °C. The *P. album* strains also exhibited different reverse colors on Potato Dextrose Agar medium (PDA) according to their subclade: most of the strains were orange-brown in subclade 1, all strains were dark brown in subclade 2 and all strains were white in subclade 3. Tsang et al. (2016) therefore concluded that further investigations would position subclades 2 and 3 at a species level. Parker et al. (2022) very recently transferred the *P. album* subclade 3 to the new species *P. torokii* on the basis of phylogenetic and morphological features, pointing out the different shape of conidia produced by *P. torokii* in comparison with *P. album*. However, they did not mention any difference in reverse color of the colonies on PDA medium, probably because they only studied *P. album* strains belonging to subclade 3.

Parengyodontium album and *P. americanum* species have been described in the context of medical studies. *Parengyodontium* album is regarded as an opportunistic human pathogen

(Augustinsky et al. 1990; Macêdo et al. 2007). Tsang et al. (2016) reported that only *P. album* subclade 2 strains were involved in deep-seated infections, while subclade 1 and 3 strains were only involved in superficial body sites. *Parengyodontium americanum* strains were recovered from clinical samples of confirmed coccidiomycoses cases without determining if these strains were sampling contaminants or the result of a co-infection with *Coccidioides* spp (Teixeira et al. 2020). Regarding the susceptibility of *P. album* to different antifungal agents used in a medical environment, susceptibilities differed not only between antifungals, but also between *P. album* subclades and even among strains belonging to the same subclade (Tsang et al. 2016). This result was particularly observed for azoles, one of the largest classes of antifungal agents in clinical use (Odds et al. 2003).

While *Parengyodontium album* and *P. americanum* were initially described in a medical context, *Parengyodontium album* is a species that is widely distributed in the environment. It has been isolated from plants (Belfiori et al. 2021; Lucero et al. 2006; Wu et al. 2013), soil (Kachuei et al. 2012; Ma et al. 2013), and especially marine environments including substrates ranging from coastal plants (Liu et al. 2021) and marine sediments (Khusnullina et al. 2018) to sea water (Pindi 2012). Incidentally, the *P. torokii* holotype was isolated from the Mars 2020 spacecraft assembly facility. One of the most original contexts in which *P. album* is frequently encountered is in cultural heritage, often in monuments suffering from deterioration, but also in other contexts (Leplat et al. 2020a). This fungal species has been recovered on monuments (Gorbushina and Petersen 2000; Ponizovskaya et al. 2019) and on artworks conserved in museums or libraries (Borrego and Molina 2019; Principi et al. 2011). Materials as various as stone, wall paintings, plaster, brick, glass, wood or paper have been affected by the presence of *P. album* (Jurado et al. 2021; Koziróg et al. 2014; Piotrowska et al. 2014; Principi et al. 2011; Schabereiter-Gurtner et al. 2001; Trovão et al. 2019). In addition, *P. album* has also been frequently isolated from the air of hypogean sites (Saarela et al. 2004), and notably in

Paleolithic decorated caves (Dominguez-Moñino et al. 2021; Leplat et al. 2019; Liñán et al. 2018). The similarity between these cultural sites, like in the marine environment, is the presence of humid salty conditions that are favorable for the growth of these fungal species (Leplat et al. 2020a). When found in relation to the deterioration process of monuments, the abundance of *P. album* varied greatly from insignificant amounts to it being the most abundant species recovered (Leplat et al. 2017; Nugari et al. 2009; Ponizovskaya et al. 2019). It is therefore important to consider possible remediation methods to deal with these species.

This study aimed to characterize the diversity of *Parengyodontium* spp. strains isolated from the cultural heritage environment by working on a set of strains recovered from several different sites between 2004 and 2019. All these strains were identified as *P. album* based on the knowledge of morphological and/or phylogenetic features before a description of *P. torokii* became available. This set was a sample group of *Parengyodontium* spp. strains that were kept in a collection. First, the study of the phylogenetic diversity of these strains was carried out by analysis of additional DNA regions to those analyzed by Teixeira et al. (2020) and Tsang et al. (2016). Teixeira et al. (2020) used the nuclear internal transcribed spacer region (ITS) to describe *P. americanum,* while Tsang et al. (2016) used the ITS, the large subunit of nuclear ribosomal region (LSU) and the protein coding gene beta-tubulin (TUB) to describe *P. album*. This study also uses the small subunit of nuclear encoded ribosomal region (SSU), the protein coding gene translation elongation factor 1-alpha (TEF) and the largest (RPB1) and second largest (RPB2) subunits of RNA polymerase II. These phylogenetic markers are also often used when studying the *Cordycipitaceae* family (Kepler et al. 2017), and were also studied by Parker et al. (2022) for the description of *P. torokii*. Our phylogenetic study sought to identify which of the *Parengyodontium* strains defined by Tsang et al. (2016) and Parker et al. (2022) can be encountered in a cultural heritage environment. The subsequent study of the phenotypic diversity of the strains should then confirm or disprove the morphological differences noticed

between the three subclades/species. Finally, the susceptibility of *Parengyodontium* spp. strains to econazole nitrate was tested to check a possible variability in the effectiveness of remediation methods used against fungal colonization in cultural heritage. Econazole nitrate is an widely used antifungal agent in the medical field (Heel et al. 1978; Kumar et al. 2014), and is also occasionally used for the same purpose in the cultural heritage field (Leplat et al. 2017).

MATERIALS AND METHODS

Strains of Parengyodontium *spp. studied*

Eighteen *Parengyodontium* spp. *strains* isolated between 2004 and 2019 in various cultural heritage sites were considered in this study (Table 1). Fifteen of the strains were isolated from five different Paleolithic decorated caves, two were isolated from a museum and one strain was isolated from the crypt of a church. Twelve of the strains were isolated through air samplings, and six were isolated through surface samplings made with sterile swabs. The airborne strains were collected with a Duo SAS Super 360 air sampler (VWR-pbi, Milan, Italy). Fifty litres of air were collected at each sampling point using a 219-hole impactor containing malt extract agar (MEA; Merck KGaA, Darmstadt, Germany) culture media in 55 mm Petri dishes. The Petri dishes containing impacted media were then taken to the laboratory for analysis. The plates were incubated in an IPP55 incubator (Memmert GmBH + Co. KG, Büchenbach, Germany) for seven days at 24 °C. Fungi were then isolated from each other using the same culture conditions as those described before. The strain isolated through swabbing followed the same laboratory process.

The strains were preserved on MEA under paraffin oil at 4 °C. Two of the eighteen strains preserved in the collection did not grow back from the collection, but their DNA had already been extracted. The phenotypic diversity of *Parengyodontium* spp. was therefore only studied

on sixteen strains, while the phylogenic study was performed on all eighteen strains. With regard to the susceptibility test, one of the two undeveloped strains had already been tested in the past (Leplat et al. 2017). All strains except one were therefore tested for susceptibility to econazole nitrate 0.2%.

Phylogenetic study

Reference strains

The strains used by Tsang et al. (2016), Teixeira et al. (2020) and by Parker et al. (2022) were chosen as reference strains for *Parengyodontium* and *Engyodontium* genera (Table 2). For all these reference strains, any sequences related to DNA regions that were not studied in the aforementioned studies were also added whenever they were available in the NCBI GenBank database (Clark et al. 2016). The names of the fungal species were updated with the current names of the species, as defined in the Mycobank (Crous et al. 2004).

DNA extraction, PCR amplification and sequencing

Fungal DNA was extracted as described by Edel et al. (2001). Appropriate primers (Table S1) were used to amplify the nuclear ribosomal internal transcribed spacer (ITS) region, the large subunit of nuclear encoded ribosomal DNA (LSU), the small subunit of nuclear encoded ribosomal DNA (SSU), the translation elongation factor 1-alpha gene (TEF), the largest subunit of RNA polymerase II (RPB1), the second largest subunit of RNA polymerase II (RPB2) and the beta-tubulin (TUB). PCR was performed in 25 µl reactions, with 1 µl of template DNA, 1 U of Taq DNA polymerase (Invitrogen, California), 2.5 µl of 10X Taq DNA polymerase buffer, 1 µl of 2 mmol l^{-1} dNTPs (Thermo Fisher Scientific, Massachusetts) and 1.5 µl of each 10 µmol l^{-1} primer (Eurogentec, Belgium). Amplifications were performed on a PrimeG thermocycler

(Antylia Scientific, Illinois) using the following parameters: a 5-minute step at 94 °C, followed by 35 cycles of 1 min at 94 °C, 1 min at the appropriate annealing temperature for each primer pair (Table S1), 1 min at 72 °C, and a final 10-minute extension step at 72 °C. PCR products were sequenced by Genoscreen (France) using the same primer set. Generated sequences were submitted to the NCBI Genbank database.

Sequence alignment and phylogenetic analyses

The sequences generated in this study were verified with BioEdit v. 7.2.5 (Hall 1999). The sequences related to reference strains were downloaded from the NCBI GenBank database. Multiple sequence alignments for each studied DNA region were performed using the FFT-NS-i alignment strategy from the MAFFT v. 7 web server (Katoh et al. 2019). Uninformative gaps and ambiguous regions were removed using the Gblocks program v. 0.91.1 implemented in the NGPhylogeny.fr service, with the program set for a lightly stringent selection (minimum number of sequences for a conserved position: 50 % of the sequences + 1; minimum length of a block: 5; allowed gap position: "with half"; Lemoine et al. 2019; Talavera and Castresana 2007). The maximum likelihood (ML) analyses of concatenated regions were performed using the graphical interface of RAxML v. 8 set to 1000 bootstrap iterations and the GTRGAMMA substitution model (Edler et al. 2019; Stamatakis 2014). Bayesian inference (BI) analyses of concatenated regions were performed using MrBayes v. 3.2.6 implemented in PhyloSuite v. 1.2.1, based on a Markov Monte Carlo Chain (MCMC) set to two simultaneously executed runs for 10,000,000 generations with the GTRGAMMA substitution model (Ronquist et al. 2012; Zhang et al. 2020). Trees were sampled every 1000 generations, the burning fraction being set to 25 %. Generated trees were edited using MEGA X (Kumar et al. 2018).

182 ***Morphological study***

183 The macroscopic features were assessed on MEA and on Potato Dextrose Agar (PDA; VWR
184 International, Pennsylvania) after a 14-day incubation at 25 °C and 32 °C. The microscopic
185 features were assessed on MEA after a 14-day incubation at 25 °C. Observations were
186 performed with a Jenavert optical microscope (Zeiss, Germany) after treatment with
187 lactophenol cotton blue solution (Pro-Lab Diagnostics Canada). Microscopic features were
188 captured with an Lt365R digital camera (Teledyne Lumenera, Canada) using the Archimed
189 program (Microvision Instruments, France).

190

191 ***In vitro susceptibility testing to econazole nitrate***

192 The susceptibility of *Parengyodontium* spp. strains to econazole nitrate 0.2 % (CTS France,
193 France) was tested by disk diffusion method on MEA. The plates were inoculated with a fungal
194 suspension of the tested strains with one strain per plate. The fungal suspensions were prepared
195 from fresh cultures in sterile water supplemented with triton 0.005 % (Thermo Fisher Scientific,
196 Massachusetts). Then a cellulose disc (diameter = 6 mm, BioMerieux, France) soaked in
197 econazole nitrate 0.2 % was laid on each plate and the plates were incubated at 25 °C for seven
198 days. The diameter of the inhibition zones outside the disk was measured in millimetres.
199 Duplicate tests were carried out for all strains. A control was performed for all strains with a
200 cellulose disk soaked in sterile water.

201

202 ***Statistical analysis***

203 The growth rates of the strains on MEA and PDA media at 25 °C as well as the results of
204 susceptibility tests were analysed using analysis of variance (ANOVA) implemented in R 4.0.1
205 (package stats; function aov; Chambers 2017; R Core Team 2021). The growth rates were
206 subjected to a power transformation to ensure the normality and the variance equality of the

data (package car; function powerTransform; Weisberg 2013), while the results of the susceptibility tests were subjected to a logarithmic transformation. The strain species and the medium were used as quantitative variables in the first ANOVA model (1), with the growth rate used as the quantitative variable. The strain number and the strain species were used as qualitative variables in the two subsequent ANOVA models (2 and 3), where the size of the inhibition halo was the quantitative variable. The two qualitative variables could not therefore be used in the same model because the variables are redundant when studied together, each different strain belonging to just one species.

$$Growth\ rate = \mu + Strain\ species_i + Medium_j + Strain\ species_i{:}Medium_j + \varepsilon_{ijk} \quad (1)$$

Where μ is a constant, *Strain species* is the effect of each species (i = 1, 2), *Medium* is the effect of each medium (j=1, 2), *Strain species:Medium* is the effect of the interaction between the two variables and ε is the residual error.

$$Inhibition\ halo\ size = \mu + Strain\ number_i + \varepsilon_{ij} \quad (2)$$

Where μ is a constant, *Strain number* is the effect of each studied strain (i = 1, 2, …, 17) and ε is the residual error.

$$Inhibition\ halo\ size = \mu + Strain\ species_i + \varepsilon_{ij} \quad (3)$$

Where μ is a constant, *Strain species* is the effect of each *P. album* subclade (i = 1, 2) and ε is the residual error.

The ANOVA tests were completed by *post hoc* Tukey's HSD analysis to rank the different means (package multcomp; function cld; Piepho 2004). All the tests performed in this study were carried out using $\alpha = 5$ %.

RESULTS

Phylogenetic study

The phylogenetic studies of the eighteen strains isolated from cultural heritage environment among forty-three taxa through both maximum likelihood and Bayesian inference confirmed their affiliation to *Parengyodontium* spp. (Fig. 1). Eleven of the strains were classified as *P. album* subclade 1, while the seven remaining strains were classified as *P. torokii*. None of the strains were classified as *P. album* subclade 2. The simultaneous use of the seven phylogenetic loci also highlighted some extent of variability inside *P. album* subclade 1 and *P. torokii*.

The sequencing of TEF locus failed for all the strains belonging to *P. torokii* clade because of the production of multiple bands by the PCR reaction under the experimental conditions of the study, while these conditions allowed a correct sequencing for all the strains belonging to *P. album* subclade 1.

Regarding the distribution of *P. album* subclade 1 and *P. torokii*, the two species had been isolated through both surface samplings and air samplings. The two species were isolated several times from the same location on the same date: for example, LRMH C325 (belonging to *P. torokii*) and LRMH C327 (belonging to *P. album*) were both isolated through surface sampling in the Chauvet cave during the January 2019 campaign. Similarly, *P. album* subclade 1 and *P. torokii* were identified among the 9 strains isolated at the same time through air sampling in the Cosquer cave. Nevertheless, *P. album* subclade 1 was dominant, representing 7 of the 9 strains isolated in the cave. Finally, all the strains that were not isolated from caves,

i.e. LRMH C120, isolated from a crypt, and LRMH C267 and LRMH C268, isolated from a museum, belonged to *P. album* subclade 1.

Morphological study

Macroscopic features

The study of the macroscopic features of strains revealed common and different characteristics between *Parengyodontium album* subclade 1 and *P. torokii*, and also some intraspecific variability inside each species (Table 3; Fig 2 and 3). The most significant difference between the two species was the growth of all *P. album* strains except LRMH C268 at 32 °C on PDA, while none of the *P. torokii* strains was able to develop at this temperature. This growth remained slow, with the highest growth rate of 15.59 mm in two weeks obtained for LRMH C358, while LRMH C327 only produced unmeasurable traces. The difference between the two species was more difficult to evaluate on MEA medium, as four out of the nine studied strains of *P. album* did not grow at 32 °C. *Parengyodontium torokii* strains also failed to grow at 32 °C on MEA. The second difference between the two species was the reverse color of the colonies on MEA and PDA at 25 °C. *Parengyodontium album* and *P. torokii* reverses displayed orange tints on MEA, but the color was generally intense for *P. album*, while the color was much slighter for *P. torokii*. On PDA, the *P. album* strains displayed shades ranging from slightly yellow to slightly brown, with some strains showing intensely yellow coloring, while *P. torokii* were generally white to very slightly yellow.

Inversely, common points between both species are that they were both white in color, and did not produce diffusible pigment on MEA and PDA media. The strains of both species were velvety to floccose on the two media. All the studied strains displayed radial growth on MEA and some strains did not on PDA. This is not related to the species but rather to the texture of

the colony, since the intensity of the radial growth seemed stronger on velvety strains than on floccose strains. Similarly, some of the strains of *P. album* subclade 1 and *P. torokii* produced colorless to yellow exudate on MEA and/or on PDA media. *Parengyodontium album* strains had growth rates between 31.14 and 40.53 mm in two weeks on MEA and between 22.30 and 36.90 mm on PDA, while *P. torokii* strains had growth rates between 19.80 and 36.10 mm on MEA and between 20.51 and 36.00 mm on PDA. Thus, *P. album* subclade 1 generally showed a significantly higher growth rate than *P. torokii*, but some strains of the two species grew rapidly, white other strains grew more slowly (Table S2; Fig.S1).

Microscopic features

The main microscopic difference between *P. album* subclade 1 and *P. torokii* was the shape of the conidia (Table. 4; Fig 4). In the two species, the conidia were one-celled, smooth and hyaline, but the conidia of *P. torokii* were clearly ellipsoidal to subcylindrical, while *P. album* conidia were mostly globose to subglobose, with rare examples tending towards an ellipsoidal shape. Some *P. torokii* strains were able to produce longer conidia than *P. album*: *Parengyodontium torokii* conidia were comprised in a range of 2.0 – 4.1 µm x 1.2 – 1.7 µm, while those of *P. album* ranged from 1.5 – 2.7 x 1.3 – 1.9.

Parengyodontium album subclade 1 and *P. torokii* both produce characteristic conidiogenous cells composed of an elongated basal portion and a terminal fertile zigzag-shaped portion beared by smooth, hyaline and septate vegetative hyphae. The conidiogenous cells were mostly solitary in the two species, but whorls of up to three conidiogenous cells were also observed to various extents in the majority of the studied strains. Conidiogenous cells measured 13 – 50 µm in *P. album* and 21 – 33 µm in *P. torokii*. Some *P. album* strains therefore produced longer conidiogenous cells than *P. torokii*, but with a greater degree of variability in each species.

In vitro susceptibility testing to econazole nitrate

The inhibition zones during the susceptibility tests of *Parengyodontium* spp. strains to econazole nitrate 0.2 % varied between 1.98 and 48.36 mm (Table S2; Fig. 5 and S2). *Parengyodontium torokii* strains were statistically more susceptible to econazole nitrate than *P. album* subclade 1, but there was more variability between strains when examined in closer detail. The two species contained relatively susceptible and tolerant strains to the biocide product, meaning that there was no specific link between susceptibility and species.

DISCUSSION

Occurrence of Parengyodontium *spp. strains in the cultural heritage environment*

Parengyodontium album is a fungal species of great interest in the domain of cultural heritage preservation due to its isolation from various historic materials that are in some cases suffering from biodeterioration (Leplat et al. 2020a). This species has recently been recovered at sites ranging from the Florence cathedral in Italy to Paleolithic decorated show caves in Spain (Dominguez-Moñino et al. 2021; Santo et al. 2021). Despite the presence of this species in cultural heritage sites, no study to date has determined precisely which type of *P. album* strains are associated to cultural heritage, although Tsang et al. (2016) identified three subclades when they described *P. album* as the single species of *Parengyodontium* genus. Note that subclade 3 has recently been moved to the *Parengyodontium torokii* species (Parker et al. 2022). Our study of eighteen strains that had been initially identified as *P. album* proved that at least *P. album* subclade 1 and *P. torokii* can be recovered on cultural heritage sites. Moreover, both species are able to coexist in the same place at the same time. The two species were also recovered from both surface samplings and air sampling. These results suggest that the ecological

328 requirements of the two species are similar. *Parengyodontium album* is known to be well
329 adapted to humid and salty environments, since this species has been abundantly isolated from
330 marine environments (Khusnullina et al. 2018; Liu et al. 2021; Pindi 2012), and in particular in
331 the cultural heritage domain in monuments suffering from salt disorders (Ponizovskaya et al.
332 2019; Trovão et al. 2019). The majority of the strains we studied were isolated from Paleolithic
333 decorated cave environments, with only three of the eighteen strains isolated in another
334 environment, *i.e.* church crypt or museum. All of these three strains belonged to *P. album*
335 subclade 1, but additional data should be collected to understand whether this result could
336 reflect a slight difference in ecological niches between *P. album* subclade 1 and *P. torokii*. No
337 *P. album* subclade 2 strain was identified among the eighteen strains studied. Interestingly, this
338 was the only subclade involved in deep-seated infection among the panel of strains studied by
339 Tsang et al. (2016) during the description of the genus *Parengyodontium*, while the two other
340 subclades were only involved in infections at superficial body sites. These results could suggest
341 some kind of adaptation of this subclade as a human pathogen, as observed for other fungal taxa
342 (De Hoog et al. 1998; Rokas et al. 2020). Tsang et al. (2016) noted that only the strains
343 belonging to subclade 2 were able to grow at temperatures above 35 °C, while *P. album*
344 subclade 1 and *P. torokii* were not. In general, the fungi that cause systemic disease must be
345 able to grow and multiply at 37 °C (Kobayashi 1996).

346

347 ***Phenotypic differences and similarities between* P. album *and* P. torokii**

348 The difference in the capability to grow above 35 °C between *P. album* subclade 2, *P. album*
349 subclade 1 and *P. torokii* raises the issue of the morphological differences between the three
350 subclades/species. Tsang et al. (2016) considered the three subclades of *P. album* and described
351 them as potential cryptic species given the significant phylogenetic differences obtained
352 through the study of ITS, LSU and TUB markers and the lack of morphological differences. In

353 our study, the additional use of SSU, TEF, RPB1 and RPB2 markers confirmed the differences
354 between the three subclades/species and highlighted some intraspecific variability within *P.*
355 *album* and *P. torokii*. However, this variability was not high enough to consider the description
356 of new species. Interestingly, the sequencing for TEF of all strains belonging to *P. torokii* failed
357 in our study because of the production of multiple parasitic bands through the PCR reaction,
358 while the sequencing of all the *P. album* was successful. The use of a hot-start Taq DNA
359 polymerase (Paul et al. 2010), as well as the use of touchdown PCR (Korbie and Mattick 2008),
360 did not resolve this issue. The fact that all sequencing of TEF failed for *P. torokii* and succeeded
361 for *P. album* was actually an indirect clue of a similar pattern in *P. torokii* strains that made
362 DNA amplification incompatible with the used primers. Despite the morphological similarity
363 between *P. album* subclades 1 and 2 and *P. torokii*, Tsang et al. (2016) pointed out some
364 possible differences, the first being the growth of *P. album* subclade 2 at temperatures above
365 35 °C, while *P. subclade* 1 and *P. torokii* did not grow at temperatures above 31 °C. The second
366 difference was the reverse color of the colonies on PDA medium: *P. album* subclade 1 strains
367 were in general orange-brown, *P. album* subclade 2 strains were dark brown and *P. torokii*
368 strains were white. Parker et al. (2022) also noticed that *P. torokii* conidia were subcylindrical
369 to ellipsoidal, while *P. album* conidia were globose. Unlike Tsang et al. (2016), eight out of the
370 nine *P. album* subclade 1 strains we inspected were able to slowly develop on PDA medium at
371 32 °C, while none of the seven *P. torokii* strains grew in the same conditions. Intraspecific
372 variability in fungal growth according to temperature is known in several fungal taxa (Möller
373 et al. 1996; Van Long et al. 2021). In some cases, this variability was linked to geographic
374 location and was also supported by phylogenetic variability (Möller et al. 1996), while in other
375 cases there was no clear relationship between growth parameters and ecological characteristics
376 or genetically distinct populations (Van Long et al. 2021). The difference between our results
377 and those of Tsang et al. (2016) cannot be explained by the geographic location of the strains,

as Tsang et al. (2016) studied *P. album* subclade 1 strains isolated from different parts of the world. Similarly, no clear phylogenetic difference occurred between the strains. This characteristic should therefore be studied in greater depth because it could be an easier way to morphologically differentiate *P. album* subclade 1 from *P. torokii*. We also observed some color differences between *P. album* and *P. torokii* on the reverse of the colonies grown on PDA medium. As noticed by Tsang et al. (2016), *P. torokii* were white in general, with some tending to be slightly yellow. The reverse colors of *P. album* strains were more marked on PDA medium although brown coloring was not as intense as the coloring reported by Tsang et al. (2016). The same phenomenon seemed to occur on MEA medium, where *P. album* showed more intense orange shades than *P. torokii*. It is difficult to evaluate this characteristic as a means to clearly differentiate between the two species. Finally, our observations confirmed those of Parker et al. (2022) regarding the shape of conidia: *P. album* conidia were globose to subglobose while *P. torokii* were ellipsoidal to subcylindrical; this is the easiest microscopic feature available to distinguish *P. torokii* from *P. album*.

Susceptibility of Parengyodontium spp. to the biocide product used in the cultural heritage domain

Econazole nitrate is a fungicide belonging to the imidazole family and is generally used in a medical context (Firooz et al. 2015; Terrell 1999). It is also used as an antifungal agent in the cultural heritage domain, and is mainly used in France (Billerbeck et al. 2002; Rakotonirainy et al. 1999), with scarce references to its utilization in other parts of the world (Fabbri and Pretelli 2014). This antifungal agent was tested because the strain LRMH C120, identified as *P. album* subclade 1, had proved tolerant to this product in a previous study about the fungal contamination of the crypt vault at Saint-Savin-sur-Gartempe Abbey church (Leplat et al. 2017). The susceptibility of the studied strains to econazole nitrate 0.2% was found to be highly

variable and was not species dependent; some strains were relatively tolerant and others susceptible in both *P. album* and *P. torokii*. This result has already been observed in other fungal taxa where strains of the same species expressed different susceptibilities toward azole products in general and to econazole in particular (Choukri et al. 2014; Hammer et al. 2000; Hassan et al. 2020). Tsang et al. (2016) tested the susceptibility of *P. album* to various azoles compounds excluding econazole, and found different results according to the compound, the subclade and even the strain considered. Strains that we had isolated at the same place and time had different susceptibilities to econazole nitrate: one of the two *P. album* strains recovered from the Bastia museum in December 2016 was strongly susceptible to econazole nitrate 0.2 %, while the other was relatively tolerant. These results highlight the importance of checking the susceptibility of fungal strains before applying a treatment, especially in a context such as cultural heritage preservation. This verification is necessary to ensure the efficiency of the treatment, especially since the use of such chemical products is increasingly questioned for environmental and health reasons (Dresler et al. 2017; Kakakhel et al. 2019).

In conclusion, this study showed that the two species *Parengyodontium album* subclade 1 and *P. torokii* can be recovered from cultural heritage sites and can occur in the same time in the same site. The morphological study showed that most of the strain of *P. album* subclade 1 were able to slowly grow at 32 °C, while none of the *P. torokii* strains were. The shape of the microconidia was also different between the two species. The study of the susceptibility of the recovered strains to econazole nitrate 0.2 % showed that some strains were relatively tolerant and others relatively susceptible in the two species. These results highlight the importance of checking the susceptibility of fungal strains before applying a treatment.

427 **ACKNOWLEDGMENTS**

428 The OPerCul workstation used to perform the robustness calculations for the phylogenetic
429 studied was supported by the Paris Ile-de-France Region – DIM “Matériaux anciens et
430 patrimoniaux”.

431 We thank Joanna Lignot for English language editing.

LITERATURE CITED

Augustinsky J, Kammeyer P, Husain A, Dehoog G, Libertin C. 1990. *Engyodontium album* endocarditis. *Journal of clinical microbiology* 28(6):1479-1481.

Belfiori B, Rubini A, Riccioni C. 2021. Diversity of endophytic and pathogenic fungi of saffron (*Crocus sativus*) plants from cultivation sites in Italy. *Diversity* 13(11):535.

Billerbeck V, Roques C, Orial G, Perret F, Morin C, Pizano L, Sire M-A. 2002. Biodétérioration d'oeuvre picturales: indentification des micromycètes responsables et traitement proposé. *Matériaux & Techniques* 90(7-8):31-36.

Borrego S, Molina A. 2019. Fungal assessment on storerooms indoor environment in the National Museum of Fine Arts, Cuba. *Air Quality, Atmosphere & Health* 12:1373-1385.

Castlebury LA, Rossman AY, Gi-Ho S, Hyten AS, Spatafora JW. 2004. Multigene phylogeny reveals new lineage for *Stachybotrys chartarum*, the indoor air fungus. *Mycological Research* 108(8):864-872.

Chambers JM. 2017. Linear models. In: Chambers JM, Hastie TJ, eds. Statistical models in S. London (United Kingdom): Routledge. p. 95-144.

Choukri F, Benderdouche M, Sednaoui P. 2014. *In vitro* susceptibility profile of 200 recent clinical isolates of *Candida* spp. to topical antifungal treatments of vulvovaginal candidiasis, the imidazoles and nystatin agents. *Journal de mycologie médicale* 24(4):303-307.

Clark K, Karsch-Mizrachi I, Lipman DJ, Ostell J, Sayers EW. 2016. GenBank. *Nucleic Acids Research* 44(D1):D67-D72.

Crous PW, Gams W, Stalpers JA, Robert V, Stegehuis G. 2004. MycoBank: an online initiative to launch mycology into the 21st century. *Studies in Mycology* 50(1):19-22.

455 De Hoog G, Bowman B, Graser Y, Haase G, El Fari M, Melzer-Krick B, Untereiner W. 1998.
456 Molecular phylogeny and taxonomy of medically important fungi. *Medical mycology*
457 36:52-56.
458 De Hoog GS. 1978. Notes some fungicolous Hyphomycetes and their relatives. *Persoonia*
459 10(1):33-81.
460 Dominguez-Moñino I, Jurado V, Rogerio-Candelera MA, Hermosin B, Saiz-Jimenez C. 2021.
461 Airborne fungi in show caves from southern Spain. *Applied Sciences* 11(11):5027.
462 Dresler C, Saladino ML, Demirbag C, Caponetti E, Martino DFC, Alduina R. 2017.
463 Development of controlled release systems of biocides for the conservation of cultural
464 heritage. *International Biodeterioration & Biodegradation* 125:150-156.
465 Edel V, Steinberg C, Gautheron N, Recorbet G, Alabouvette C. 2001. Genetic diversity of
466 *Fusarium oxysporum* populations isolated from different soils in France. *FEMS*
467 *Microbiology Ecology* 36:61-71.
468 Edler D, Klein J, Antonelli A, Silvestro D. 2019. raxmlGUI 2.0 beta: a graphical interface and
469 toolkit for phylogenetic analyses using RAxML. *BioRxiv*:800912.
470 Fabbri K, Pretelli M. 2014. Heritage buildings and historic microclimate without HVAC
471 technology: Malatestiana Library in Cesena, Italy, UNESCO Memory of the World.
472 *Energy and Buildings* 76:15-31.
473 Firooz A, Nafisi S, Maibach HI. 2015. Mini review: Novel drug delivery strategies for
474 improving econazole antifungal action. *International Journal of Pharmaceutics*
475 495:599-607.
476 Gardes M, Bruns TD. 1993. ITS primers with enhanced specificity for basidiomycetes-
477 application to the identification of mycorrhizae and rusts. *Molecular Ecology* 2(2):113-
478 118.

Glass NL, Donaldson GC. 1995. Development of primer sets designed for use with the PCR to amplify conserved genes from filamentous ascomycetes. *Applied and Environmental Microbiology* 61(4):1323-1330.

Gorbushina AA, Petersen K. 2000. Distribution of microorganisms on ancient wall paintings as related to associated faunal elements. *International biodeterioration & biodegradation* 46(4):277-284.

Hall TA. 1999. BioEdit: a user-friendly biological sequence alignment editor and analysis program for Windows 95/98/NT. *Nucleic Acids Symposium Series* 41(41):95-98.

Hammer KA, Carson CF, Riley TV. 2000. In vitro activities of ketoconazole, econazole, miconazole, and *Melaleuca alternifolia* (tea tree) oil against *Malassezia* species. *Antimicrobial agents and chemotherapy* 44(2):467-469.

Hassan AS, Sangeetha AB, Shobana CS, Mythili A, Suresh S, Abirami B, Alharbi RA, Aloyuni SA, Abdel-Hadi A, Awad MF. 2020. In-vitro assessment of first-line antifungal drugs against *Aspergillus* spp. caused human keratomycoses. *Journal of Infection and Public Health* 13(12):1907-1911.

Heel RC, Brogden RN, Speight TM, Avery GS. 1978. Econazole: A review of its antifungal activity and therapeutic efficacy. *Drugs* 16(3):177-201.

Jurado V, Gonzalez-Pimentel JL, Hermosin B, Saiz-Jimenez C. 2021. Biodeterioration of Salón de Reinos, Museo Nacional del Prado, Madrid, Spain. *Applied Sciences* 11(19):8858.

Kachuei R, Emami M, Naeimi B, Diba K. 2012. Isolation of keratinophilic fungi from soil in Isfahan province, Iran. *Journal de Mycologie Medicale* 22(1):8-13.

Kakakhel MA, Wu F, Gu J-D, Feng H, Shah K, Wang W. 2019. Controlling biodeterioration of cultural heritage objects with biocides: A review. *International Biodeterioration & Biodegradation* 143:104721.

503 Katoh K, Rozewicki J, Yamada KD. 2019. MAFFT online service: multiple sequence
504 alignment, interactive sequence choice and visualization. *Briefings in Bioinformatics*
505 20(4):1160-1166.
506 Kepler RM, Luangsa-Ard JJ, Hywel-Jones NL, Quandt CA, Sung G-H, Rehner SA, Aime MC,
507 Henkel TW, Sanjuan T, Zare R. 2017. A phylogenetically-based nomenclature for
508 Cordycipitaceae (Hypocreales). *IMA fungus* 8(2):335-353.
509 Khusnullina A, Bilanenko E, Kurakov A. 2018. Microscopic fungi of White Sea sediments.
510 *Contemporary Problems of Ecology* 11(5):503-513.
511 Kobayashi GS. 1996. Disease mechanisms of fungi. In: Baron S, ed. Medical Microbiology.
512 4th edition. Galveston (USA): University of Texas Medical Branch at Galveston.
513 Korbie DJ, Mattick JS. 2008. Touchdown PCR for increased specificity and sensitivity in PCR
514 amplification. *Nature protocols* 3(9):1452-1456.
515 Koziróg A, Otlewska A, Piotrowska M, Rajkowska K, Nowicka-Krawczyk P, Hachułka M,
516 Wolski GJ, Gutarowska B, Kunicka-Styczyńska A, Libudzisz Z et al. 2014. Colonising
517 organisms as a biodegradation factor affecting historical wood materials at the former
518 concentration camp of Auschwitz II – Birkenau. *International Biodeterioration &*
519 *Biodegradation* 86:171-178.
520 Kumar L, Verma S, Bhardwaj A, Vaidya S, Vaidya B. 2014. Eradication of superficial fungal
521 infections by conventional and novel approaches: a comprehensive review. *Artificial*
522 *cells, nanomedicine, and biotechnology* 42(1):32-46.
523 Kumar S, Stecher G, Li M, Knyaz C, Tamura K. 2018. MEGA X: molecular evolutionary
524 genetics analysis across computing platforms. *Molecular Biology and Evolution*
525 35(6):1547-1549.

526 Lemoine F, Correia D, Lefort V, Doppelt-Azeroual O, Mareuil F, Cohen-Boulakia S, Gascuel
527 O. 2019. NGPhylogeny.fr: new generation phylogenetic services for non-specialists.
528 *Nucleic Acids Research* 47(W1):W260-W265.
529 Leplat J, Francois A, Bousta F. 2017. White fungal covering on the wall paintings of the Saint-
530 Savin-sur-Gartempe Abbey church crypt: A case study. *International Biodeterioration*
531 *& Biodegradation* 122:29-37.
532 Leplat J, François A, Bousta F. 2020a. *Parengyodontium album*, a frequently reported fungal
533 species in the cultural heritage environment. *Fungal Biology Reviews*.
534 Leplat J, François A, Touron S, Frouin M, Portais J-C, Bousta F. 2020b. Aerobiological
535 behavior of Paleolithic rock art sites in Dordogne (France): a comparative study in
536 protected sites ranging from rock shelters to caves, with and without public access.
537 *Aerobiologia*:1-20.
538 Leplat J, François A, Touron S, Galant P, Bousta F. 2019. Aerobiological behavior of
539 Paleolithic decorated caves: a comparative study of five caves in the Gard department
540 (France). *Aerobiologia* 35(1):105-124.
541 Liñán C, del Rosal Y, Carrasco F, Vadillo I, Benavente J, Ojeda L. 2018. Highlighting the
542 importance of transitional ventilation regimes in the management of Mediterranean
543 show caves (Nerja-Pintada system, southern Spain). *Science of The Total Environment*
544 631-632:1268-1278.
545 Liu S, Mao Y, Lu H, Zhao Y, Bilal M, Proksch P, Hu P. 2021. Two new torrubiellin derivatives
546 from the mangrove endophytic fungus *Parengyodontium album*. *Phytochemistry Letters*
547 46:149-152.
548 Liu YJ, Whelen S, Hall BD. 1999. Phylogenetic relationships among ascomycetes: evidence
549 from an RNA polymerse II subunit. *Molecular Biology and Evolution* 16(12):1799-
550 1808.

551 Lucero M, Barrow J, Osuna P, Reyes I. 2006. Plant–fungal interactions in arid and semi-arid
552 ecosystems: Large-scale impacts from microscale processes. *Journal of arid*
553 *environments* 65(2):276-284.
554 Ma A, Zhuang X, Wu J, Cui M, Lv D, Liu C, Zhuang G. 2013. Ascomycota members dominate
555 fungal communities during straw residue decomposition in arable soil. *PloS one*
556 8(6):e66146.
557 Macêdo DPC, Neves RP, Souza-Motta CMd, Magalhães OMC. 2007. *Engyodontium album*
558 fungaemia: the first reported case. *Brazilian Journal of Microbiology* 38(1):110-112.
559 Matheny PB, Liu YJ, Ammirati JF, Hall BD. 2002. Using RPB1 sequences to improve
560 phylogenetic inference among mushrooms (Inocybe, Agaricales). *American Journal of*
561 *Botany* 89(4):688-698.
562 Möller C, Weber G, Dreyfuss M. 1996. Intraspecific diversity in the fungal species
563 *Chaunopycnis alba*: implications for microbial screening programs. *Journal of*
564 *industrial microbiology and biotechnology* 17(5-6):359-372.
565 Nugari MP, Pietrini AM, Caneva G, Imperi F, Visca P. 2009. Biodeterioration of mural
566 paintings in a rocky habitat: The Crypt of the Original Sin (Matera, Italy). *International*
567 *Biodeterioration & Biodegradation* 63:705-711.
568 Odds FC, Brown AJ, Gow NA. 2003. Antifungal agents: mechanisms of action. *Trends in*
569 *microbiology* 11(6):272-279.
570 Parker CW, Teixeira MdM, Singh NK, Raja HA, Cank KB, Spigolon G, Oberlies NH, Barker
571 BM, Stajich JE, Mason CE et al. 2022. Genomic characterization of *Parengyodontium*
572 *torokii* sp. nov., a biofilm-forming fungus isolated from Mars 2020 assembly facility.
573 *Journal of Fungi* 8(1):66.
574 Paul N, Shum J, Le T. 2010. Hot start PCR. In: King N, ed. RT-PCR Protocols. Berlin
575 (Germany): Springer. p. 301-318.

576 Piepho H-P. 2004. An algorithm for a letter-based representation of all-pairwise comparisons.
577 *Journal of Computational and Graphical Statistics* 13(2):456-466.
578 Pindi PK. 2012. Diversity of fungi at various depths of marine water. *Research in*
579 *Biotechnology* 3(4).
580 Piotrowska M, Otlewska A, Rajkowska K, Koziróg A, Hachułka M, Nowicka-Krawczyk P,
581 Wolski GJ, Gutarowska B, Kunicka-Styczyńska A, Żydzik-Białek A. 2014. Abiotic
582 determinants of the historical buildings biodeterioration in the former Auschwitz II –
583 Birkenau concentration and extermination camp. *PLOS ONE* 9(10):e109402.
584 Ponizovskaya VB, Rebrikova NL, Kachalkin AV, Antropova AB, Bilanenko EN, Mokeeva VL.
585 2019. Micromycetes as colonizers of mineral building materials in historic monuments
586 and museums. *Fungal Biology* 123:290-306.
587 Principi P, Villa F, Sorlini C, Cappitelli F. 2011. Molecular studies of microbial community
588 structure on stained pages of Leonardo da Vinci's Atlantic Codex. *Microbial ecology*
589 61(1):214-222.
590 R Core Team RC. 2021. R: A language and environment for statistical computing. R
591 Foundation for Statistical Computing, Vienna, Austria. https://www.R-project.org/.
592 Rakotonirainy MS, Fohrer F, Flieder F. 1999. Research on fungicides for aerial disinfection by
593 thermal fogging in libraries and archives. *International biodeterioration &*
594 *biodegradation* 44(2-3):133-139.
595 Rehner S, Buckley E. 2005. A *Beauveria* phylogeny inferred from nuclear ITS and EF1-a
596 sequences: evidence for cryptic diversification and links to *Cordyceps* teleomorphs.
597 *Mycologia* 97(1):84-98.
598 Rokas A, Mead ME, Steenwyk JL, Oberlies NH, Goldman GH. 2020. Evolving moldy
599 murderers: *Aspergillus* section Fumigati as a model for studying the repeated evolution
600 of fungal pathogenicity. *PLoS pathogens* 16(2):e1008315.

601 Ronquist F, Teslenko M, Van Der Mark P, Ayres DL, Darling A, Höhna S, Larget B, Liu L,
602 Suchard MA, Huelsenbeck JP. 2012. MrBayes 3.2: efficient Bayesian phylogenetic
603 inference and model choice across a large model space. *Systematic Biology* 61(3):539-
604 542.
605 Saarela M, Alakomi H-L, Suihko M-L, Maunuksela L, Raaska L, Mattila-Sandholm T. 2004.
606 Heterotrophic microorganisms in air and biofilm samples from Roman catacombs, with
607 special emphasis on actinobacteria and fungi. *International Biodeterioration &*
608 *Biodegradation* 54(1):27-37.
609 Santo AP, Cuzman OA, Petrocchi D, Pinna D, Salvatici T, Perito B. 2021. Black on white:
610 microbial growth darkens the external marble of florence cathedral. *Applied Sciences*
611 11(13):6163.
612 Schabereiter-Gurtner C, Piñar G, Lubitz W, Rölleke S. 2001. Analysis of fungal communities
613 on historical church window glass by denaturing gradient gel electrophoresis and
614 phylogenetic 18S rDNA sequence analysis. *Journal of Microbiological Methods*
615 47(3):345-354.
616 Stamatakis A. 2014. RAxML version 8: a tool for phylogenetic analysis and post-analysis of
617 large phylogenies. *Bioinformatics* 30(9):1312-1313.
618 Talavera G, Castresana J. 2007. Improvement of phylogenies after removing divergent and
619 ambiguously aligned blocks from protein sequence alignments. *Systematic Biology*
620 56(4):564-577.
621 Teixeira MdM, Muszewska A, Travis J, Moreno LF, Ahmed S, Roe C, Mead H, Steczkiewicz
622 K, Lemmer D, de Hoog S et al. . 2020. Genomic characterization of *Parengyodontium*
623 *americanum* sp. nov. *Fungal Genetics and Biology*:103351.
624 Terrell CL. 1999. Antifungal Agents. Part II. The Azoles. *Mayo Clinic Proceedings* 74(1):78-
625 100.

626 Trovão J, Portugal A, Soares F, Paiva DS, Mesquita N, Coelho C, Pinheiro AC, Catarino L, Gil
627 F, Tiago I. 2019. Fungal diversity and distribution across distinct biodeterioration
628 phenomena in limestone walls of the old cathedral of Coimbra, UNESCO World
629 Heritage Site. *International Biodeterioration & Biodegradation* 142:91-102.
630 Tsang C-C, Chan JFW, Pong W-M, Chen JHK, Ngan AHY, Cheung M, Lai CKC, Tsang DNC,
631 Lau SKP, Woo PCY. 2016. Cutaneous hyalohyphomycosis due to *Parengyodontium*
632 *album* gen. et comb. nov. *Medical Mycology* 54(7):699-713.
633 Van Long NN, Rigalma K, Jany J-L, Mounier J, Vasseur V. 2021. Intraspecific variability in
634 cardinal growth temperatures and water activities within a large diversity of *Penicillium*
635 *roqueforti* strains. *Food Research International* 148:110610.
636 Vilgalys R, Hester M. 1990. Rapid genetic identification and mapping of enzymatically
637 amplified ribosomal DNA from several *Cryptococcus* species. *Journal of Bacteriology*
638 172(8):4238-4246.
639 Weisberg S. 2013. Applied linear regression. Hoboken (USA): John Wiley & Sons.
640 White TJ, Bruns T, Lee SJWT, Taylor JW. 1990. Amplification and direct sequencing of fungal
641 ribosomal RNA genes for phylogenetics. In: Innis MA, Gelfand DH, Sninsky JJ, White
642 TJ, eds. PCR protocols: a guide to methods and applications. San Diego (USA):
643 Academic Press, Inc. p. 315-322.
644 Wu H, Yang H-Y, You X-L, Li Y-H. 2013. Diversity of endophytic fungi from roots of *Panax*
645 *ginseng* and their saponin yield capacities. *SpringerPlus* 2(1):1-9.
646 Zhang D, Gao F, Jakovlić I, Zou H, Zhang J, Li WX, Wang GT. 2020. PhyloSuite: an integrated
647 and scalable desktop platform for streamlined molecular sequence data management
648 and evolutionary phylogenetics studies. *Molecular Ecology Resources* 20(1):348-355.
649

650 Table 1: Description of *Parengyodontium* spp. strains selected to study phylogeny, phenotypes
651 and susceptibility to econazole nitrate.

Collection number	Species	Sampling place	Sampling date	Sampling method	Preceding study referring to the strain
LRMH C057	*Parengyodontium torokii*	Lascaux cave (Nouvelle-Aquitaine, France)	12/2004	Air sampling	(-)
LRMH C120*	*P. album*	Crypt of Saint-Savin-sur Gartempe Abbey church (Nouvelle-Aquitaine, France)	11/2015	Surface sampling	(Leplat et al. 2017)
LRMH C133	*P. torokii*	Chauvet cave (Auvergne-Rhône-Alpes, France)	03/2016	Surface sampling	(-)
LRMH C243	*P. torokii*	Pair-non-Pair cave (Nouvelle-Aquitaine, France)	10/2016	Air sampling	(-)
LRMH C267	*P. album*	Bastia Museum	12/2016	Surface sampling	(-)
LRMH C268	*P. album*	Bastia Museum	12/2016	Surface sampling	(-)
LRMH C325	*P. torokii*	Chauvet cave (Auvergne-Rhône-Alpes, France)	01/2019	Surface sampling	(-)
LRMH C327	*P. album*	Chauvet cave (Auvergne-Rhône-Alpes, France)	01/2019	Surface sampling	(-)
LRMH C343*	*P. album*	Cosquer cave (Provence-Alpes-Côte d'Azur, France)	07/2019	Air sampling	(-)
LRMH C345	*P. album*	Cosquer cave (Provence-Alpes-Côte d'Azur, France)	07/2019	Air sampling	(-)
LRMH C346	*P. album*	Cosquer cave (Provence-Alpes-Côte d'Azur, France)	07/2019	Air sampling	(-)
LRMH C349	*P. album*	Cosquer cave (Provence-Alpes-Côte d'Azur, France)	07/2019	Air sampling	(-)
LRMH C350	*P. album*	Cosquer cave (Provence-Alpes-Côte d'Azur, France)	07/2019	Air sampling	(-)
LRMH C355	*P. album*	Cosquer cave (Provence-Alpes-Côte d'Azur, France)	07/2019	Air sampling	(-)
LRMH C356	*P. torokii*	Cosquer cave (Provence-Alpes-Côte d'Azur, France)	07/2019	Air sampling	(-)
LRMH C357	*P. torokii*	Cosquer cave (Provence-Alpes-Côte d'Azur, France)	07/2019	Air sampling	(-)
LRMH C358	*P. album*	Cosquer cave (Provence-Alpes-Côte d'Azur, France)	07/2019	Air sampling	(-)
LRMH C364	*P. torokii*	Pigeonnier cave (Nouvelle-Aquitaine, France)	10/2016	Air sampling	(Leplat et al. 2020b)

652 * Strains only included in the phylogenetic study; the preserved strains did not grow back from the collection tubes and were therefore excluded
653 from the phenotype study.

Table 2: Fungal taxa used in the phylogenetic study.

Species	*Parengyodontium album* subclade	Collection number	ITS	SSU	LSU	TEF	RPB1	RPB2	TUB	Reference study
Parengyodontium album	Subclade 1	HKU48	LC092879	(-)	LC092898	(-)	(-)	(-)	LC092917	(Tsang et al. 2016)
P. album	Subclade 1	CBS 504.83	LC092880	(-)	LC092899	LC425535	(-)	(-)	LC092918	(Tsang et al. 2016)
P. album	Subclade 1	CBS 570.71	LC092881	(-)	LC092900	LC425551	(-)	(-)	LC092919	(Tsang et al. 2016)
P. album	Subclade 1	CBS 836.71	LC092882	(-)	LC092901	LC382178	(-)	(-)	LC092920	(Tsang et al. 2016)
P. album	Subclade 1	CBS 121919	LC092883	(-)	LC092902	LC425536	(-)	(-)	LC092921	(Tsang et al. 2016)
P. album	Subclade 1	UAMH 1441	LC092884	(-)	LC092903	LC425557	(-)	(-)	LC092922	(Tsang et al. 2016)
P. album	Subclade 1	UAMH 10043	LC092885	(-)	LC092904	LC425537	(-)	(-)	LC092923	(Tsang et al. 2016)
P. album	Subclade 1	NRRL 2312	LC092886	(-)	LC092905	(-)	(-)	(-)	LC092924	(Tsang et al. 2016)
P. album	Subclade 2	IHEM 4198	LC092887	(-)	LC092906	LC425561	(-)	(-)	LC092925	(Tsang et al. 2016)
P. album	Subclade 2	UAMH 4512	LC092888	(-)	LC092907	LC382182	(-)	(-)	LC092926	(Tsang et al. 2016)
P. album	Subclade 2	UAMH 8313	LC092889	(-)	LC092908	(-)	(-)	(-)	LC092927	(Tsang et al. 2016)
P. album	Subclade 2	UAMH 11234	LC092890	(-)	LC092909	LC425560	(-)	(-)	LC092928	(Tsang et al. 2016)
P. album	**Subclade 1**	**LRMH C120**	**KX821728**	**OL913902**	**OL981475**	**OM201767**	**OL904974**	**OL904992**	**OM201750**	**This study**
P. album	**Subclade 1**	**LRMH C267**	**OL913885**	**OL913905**	**OL981478**	**OM201768**	**OL904977**	**OL904995**	**OM201753**	**This study**
P. album	**Subclade 1**	**LRMH C268**	**OL913886**	**OL913906**	**OL981479**	**OM201769**	**OL904978**	**OL904996**	**OM201754**	**This study**
P. album	**Subclade 1**	**LRMH C327**	**OL913888**	**OL913908**	**OL981481**	**OM201770**	**OL904980**	**OL904998**	**OM201756**	**This study**
P. album	**Subclade 1**	**LRMH C343**	**OL913889**	**OL913909**	**OL981482**	**OM201771**	**OL904981**	**OL904999**	**OM201757**	**This study**
P. album	**Subclade 1**	**LRMH C345**	**OL913890**	**OL913910**	**OL981483**	**OM201772**	**OL904982**	**OL905000**	**OM201758**	**This study**
P. album	**Subclade 1**	**LRMH C346**	**OL913891**	**OL913911**	**OL981484**	**OM201773**	**OL904983**	**OL905001**	**OM201759**	**This study**
P. album	**Subclade 1**	**LRMH C349**	**OL913892**	**OL913912**	**OL981485**	**OM201774**	**OL904984**	**OL905002**	**OM201760**	**This study**
P. album	**Subclade 1**	**LRMH C350**	**OL913893**	**OL913913**	**OL981486**	**OM201775**	**OL904985**	**OL905003**	**OM201761**	**This study**
P. album	**Subclade 1**	**LRMH C355**	**OL913894**	**OL913914**	**OL981487**	**OM201776**	**OL904986**	**OL905004**	**OM201762**	**This study**
P. album	**Subclade 1**	**LRMH C358**	**OL913897**	**OL913917**	**OL981490**	**OM201777**	**OL904989**	**OL905007**	**OM201765**	**This study**
Parengyodontium americanum	(-)	AZ2	KY683770	(-)	(-)	(-)	(-)	(-)	(-)	(Teixeira et al. 2020)
P. americanum	(-)	CA11	KY683771	(-)	(-)	(-)	(-)	(-)	(-)	(Teixeira et al. 2020)
P. americanum	(-)	CA13	KY683772	(-)	(-)	(-)	(-)	(-)	(-)	(Teixeira et al. 2020)
P. americanum	(-)	CA19	KY683773	(-)	(-)	(-)	(-)	(-)	(-)	(Teixeira et al. 2020)
P. americanum	(-)	CA21	KY683774	(-)	(-)	(-)	(-)	(-)	(-)	(Teixeira et al. 2020)
Parengyodontium torokii	Subclade 3	NRLL 64203*	MT704894	(-)	(-)	(-)	(-)	(-)	(-)	(Parker et al. 2022)
P. torokii	Subclade 3	CBS 368.72	LC092891	(-)	LC092910	LC382183	(-)	(-)	LC092929	(Tsang et al. 2016)
P. torokii	Subclade 3	UAMH 9836	LC092892	(-)	LC092911	LC382184	(-)	(-)	LC092930	(Tsang et al. 2016)

P. torokii	**Subclade 3**	**LRMH C057**	**OL913882**	**OL913901**	**OL981474**	**(-)**	**OL904973**	**OL904991**	**OM201749**	**This study**
P. torokii	**Subclade 3**	**LRMH C133**	**OL913883**	**OL913903**	**OL981476**	**(-)**	**OL904975**	**OL904993**	**OM201751**	**This study**
P. torokii	**Subclade 3**	**LRMH C243**	**OL913884**	**OL913904**	**OL981477**	**(-)**	**OL904976**	**OL904994**	**OM201752**	**This study**
P. torokii	**Subclade 3**	**LRMH C325**	**OL913887**	**OL913907**	**OL981480**	**(-)**	**OL904979**	**OL904997**	**OM201755**	**This study**
P. torokii	**Subclade 3**	**LRMH C356**	**OL913895**	**OL913915**	**OL981488**	**(-)**	**OL904987**	**OL905005**	**OM201763**	**This study**
P. torokii	**Subclade 3**	**LRMH C357**	**OL913896**	**OL913916**	**OL981489**	**(-)**	**OL904988**	**OL905006**	**OM201764**	**This study**
P. torokii	**Subclade 3**	**LRMH C364**	**OL913898**	**OL913918**	**OL981491**	**(-)**	**OL904990**	**OL905008**	**OM201766**	**This study**
Engyodontium rectidentatum	(-)	CBS 206.74	LC092893	(-)	LC092912	LC425553	(-)	(-)	LC092931	(Tsang et al. 2016)
E. rectidentatum	(-)	CBS 547.82	LC092894	(-)	LC092913	LC425544	(-)	(-)	LC092932	(Tsang et al. 2016)
E. rectidentatum	(-)	CBS 641.74	LC092895	(-)	LC092914	LC425540	(-)	(-)	(-)	(Tsang et al. 2016)
Engyodontium parvisporum	(-)	IHEM 22910	LC092896	(-)	LC092915	LC425558	(-)	(-)	LC092933	(Tsang et al. 2016)
Engyodontium aranearum	(-)	CBS 658.80	LC092897	(-)	LC092916	(-)	(-)	(-)	LC092934	(Tsang et al. 2016)

*Although Parker et al. (2022) used each one of these seven phylogenetic markers, the ITS sequence is the only locus to be specifically available in the Genbank, the other loci being included in a Whole-Genome sequence composed of 30,430,964 bp. Therefore, these loci could not be used in this study.

Table 3: Macroscopic features of the *Parangyodontium* spp. strains studied.

Strain	Size (mm)*	Color	Reverse color	Texture	Radial growth	Exudate	Size (mm)**	Size (mm)*	Color	Reverse color	Texture	Radial growth	Exudate	Size (mm)**
				MEA							PDA			
				25 °C			32 °C				25 °C			32 °C
Parengyodontium album subclade 1														
LRMH C267	34.35	White	Strongly orangey	Velvety	Strong	(-)	18.36	32.09	White	Yellow	Velvety to floccose	Slight	(-)	19.04
LRMH C268	36.31			Floccose	Slight		(-)	29.20		Yellow to slightly brown	Floccose	(-)		(-)
LRMH C327	31.52			Floccose	Slight			22.30		Yellow to slightly brown	Floccose	(-)		Traces
LRMH C345	38.04			Floccose	Slight			35.19		Yellow to slightly brown	Velvety to floccose	Slight		13.58
LRMH C346	30.08			Velvety	Strong			30.64		White to yellow	Velvety	Slight		8.55
LRMH C349	31.14			Velvety	Strong		9.45	31.24		Yellow to slightly brown	Velvety to floccose	Slight	Slight, colorless to yellow	14.78
LRMH C350	31.16			Velvety	Strong		6.12	29.76		Yellow to slightly brown	Velvety to floccose	Slight	Slight, colorless to yellow	14.53
LRMH C355	31.69			Velvety	Strong		14.06	31.25		White to yellow	Velvety to floccose	Slight	(-)	14.50
LRMH C358	40.53			Floccose	Slight	Yellow	13.57	36.9		White to slightly yellow	Floccose	(-)		15.59
Parengyodontium torkii (*Parengyodontium album* subclade 3)														
LRMH C057	33.80	White	Orangey	Floccose	Slight	(-)	(-)	36.00	White	White to slightly yellow	Floccose	Slight	(-)	(-)
LRMH C133	30.56			Floccose	Very slight	Yellow		34.44			Floccose	(-)	Colorless to yellow	
LRMH C243	26.13			Velvety to floccose	Strong			24.37			Floccose	Slight		
LRMH C325	20.60			Floccose	Slight			20.84			Floccose	(-)	(-)	
LRMH C356	33.00			Velvety	Strong	(-)		35.11			Velvety to floccose	Slight		
LRMH C357	36.10			Velvety	Strong			35.20			Velvety to floccose	Slight		
LRMH C364	19.80			Velvety	Strong			20.51			Velvety to floccose	Slight	Slight, colorless to yellow	

*The sizes at 25 °C were obtained by the mean of three replications on the same Petri dish.

**The sizes at 32 °C were obtained by the mean of the number of replications that grew (from 1 to 3) on the same Petri dish.

660 Table 4: Microscopic features of the *Parangyodontium* spp. strains studied*.

Strain	Conidiogenous cells		Conidia	
	Organization	Limit sizes measured (µm)	Shape	Limit sizes measured (µm)
		Parengyodontium album subclade 1		
LRMH C267	Mostly solitary, occasionally whorls of 2 cells	14 – 22	Globose to subglobose	2.0 – 2.2 x 1.3 – 1.9
LRMH C268	Solitary and in whorls of 2 to 3 cells	13 – 21	Globose to subglobose	1.5 – 2.1 x 1;5 – 1.9
LRMH C327	Solitary and in whorls of 2 to 3 cells	25 – 26	Subglobose to ellipsoidal	2.2 – 2.7 x 1.1 – 1.6
LRMH C345	Solitary and in whorls of 2 to 3 cells	28 – 34	Globose to subglobose	2.1 – 2.3 x 1.5 – 1.6
LRMH C346	Solitary and in whorls of 2 to 3 cells	37 – 50	Subglobose to ellipsoidal	2.0 – 2.9 x 1.7 – 1.8
LRMH C349	Solitary and in whorls of 2 cells	36 – 44	Globose to subglobose	2.1 – 2.3 x 1.5 – 1.6
LRMH C350	Solitary and in whorls of 2 to 3 cells	27 – 28	Globose to subglobose	1.9 – 2.7 x 1.3 – 1.4
LRMH C355	Solitary and in whorls of 2 cells	16 – 27	Subglobose to ellipsoidal	2.0 – 2.5 x 1.4 – 1.6
LRMH C358	Solitary and in whorls of 2 to 3 cells	33 – 40	Globose to subglobose	2.0 – 2.1 x 1.5 – 1.6
		Parengyodontium torkii (*Parengyodontium album* subclade 3)		
LRMH C057	Mostly solitary, occasionally whorls of 2 cells	26 – 28	Ellipsoidal to subcylindrical	2.2 – 3.4 x 1.4 – 1.5
LRMH C133	Mostly solitary, occasionally whorls of 2 cells	24 – 30	Ellipsoidal to subcylindrical	2.0 – 2.7 x 1.4 – 1.6
LRMH C243	Solitary and in whorls of 2 cells	21 – 33	Ellipsoidal to subcylindrical	2.1 – 2.2 x 1.4 – 1.5
LRMH C325	Solitary and in whorls of 2 to 3 cells	23 – 28	Ellipsoidal to subcylindrical	2.3 – 2.4 x 1.4 – 1.5
LRMH C356	Solitary and in whorls of 2 cells	22 – 23	Ellipsoidal to subcylindrical	2.5 – 3.0 x 1.2 – 1.4
LRMH C357	Solitary and in whorls of 2 cells	25 – 27	Ellipsoidal to subcylindrical	2.5 – 2.7 x 1.4 – 1.5
LRMH C364	Solitary and in whorls of 2 cells	25 – 27	Ellipsoidal to subcylindrical	3.1 – 4.1 x 1.5 – 1.7

661 *Only features that introduce a degree of diversity between species and/or strains are listed in the table; the features common to all strains are

662 not included.

663 **LEGENDS**

664 Figure 1: Phylogenetic studies of *Parengyodontium* spp. strains isolated from a cultural heritage
665 environment through maximum likelihood and Bayesian inference.
666 The trees were obtained from a dataset including 43 taxa leading to a concatenated alignment
667 of 4677 bp from seven nuclear regions (ITS, LSU, SSU, RPB1, RPB2, TEF and TUB). The
668 trees were rooted with *Engyodontium* clade as an outgroup. Bootstrap values greater than or
669 equal to 70 % and Bayesian posterior probabilities greater than or equal to 0.70 are located
670 close to the corresponding node. The specific strains studied are marked in bold.
671
672 Figure 2: Macroscopic features of the *Parengyodontium album* subclade 1 strains studied.
673 For each strain, growth on MEA medium is displayed on the left and growth on PDA medium
674 on the right. For each Petri dish, the recto side is displayed on the left and the reverse side on
675 the right.
676
677 Figure 3: Macroscopic features of the *Parengyodontium torokii* (*P. album* subclade 3) strains
678 studied.
679 For each strain, growth on MEA medium is displayed on the left and growth on PDA medium
680 on the right. For each Petri dish, the recto side is displayed on the left and the reverse side on
681 the right.
682
683 Figure 4: Microscopic features of *Parengyodontium* spp. strains studied.
684 Shape of microconidia: Ellipsoidal to subcylindrical conidia of *P. torokii* (a) and globose to
685 subglobose conidia of *P. album* subclade 1 (b). Size of conidiogenous cells: short
686 conidiogenous cells (c) and long conidiogenous cells (d). Organization of conidiogenous cells:
687 solitary conidiogenous cells (e) and conidiogenous cells in whorls (f and g). Scale bars: 10 µm.

688

689 Figure 5: Susceptibility of *Parengyodontium* spp. strains to econazole nitrate 0.2 %.

690 The bars display the inhibition halo size around the cellulose disc soaked in econazole nitrate.
691 The error bars were obtained by calculating the mean of two repetitions. The results regarding
692 the strain LRMH C120 were obtained from (Leplat et al. 2017).

*corresponding author e-mail: johann.leplat@culture.gouv.fr

693 Figure 1

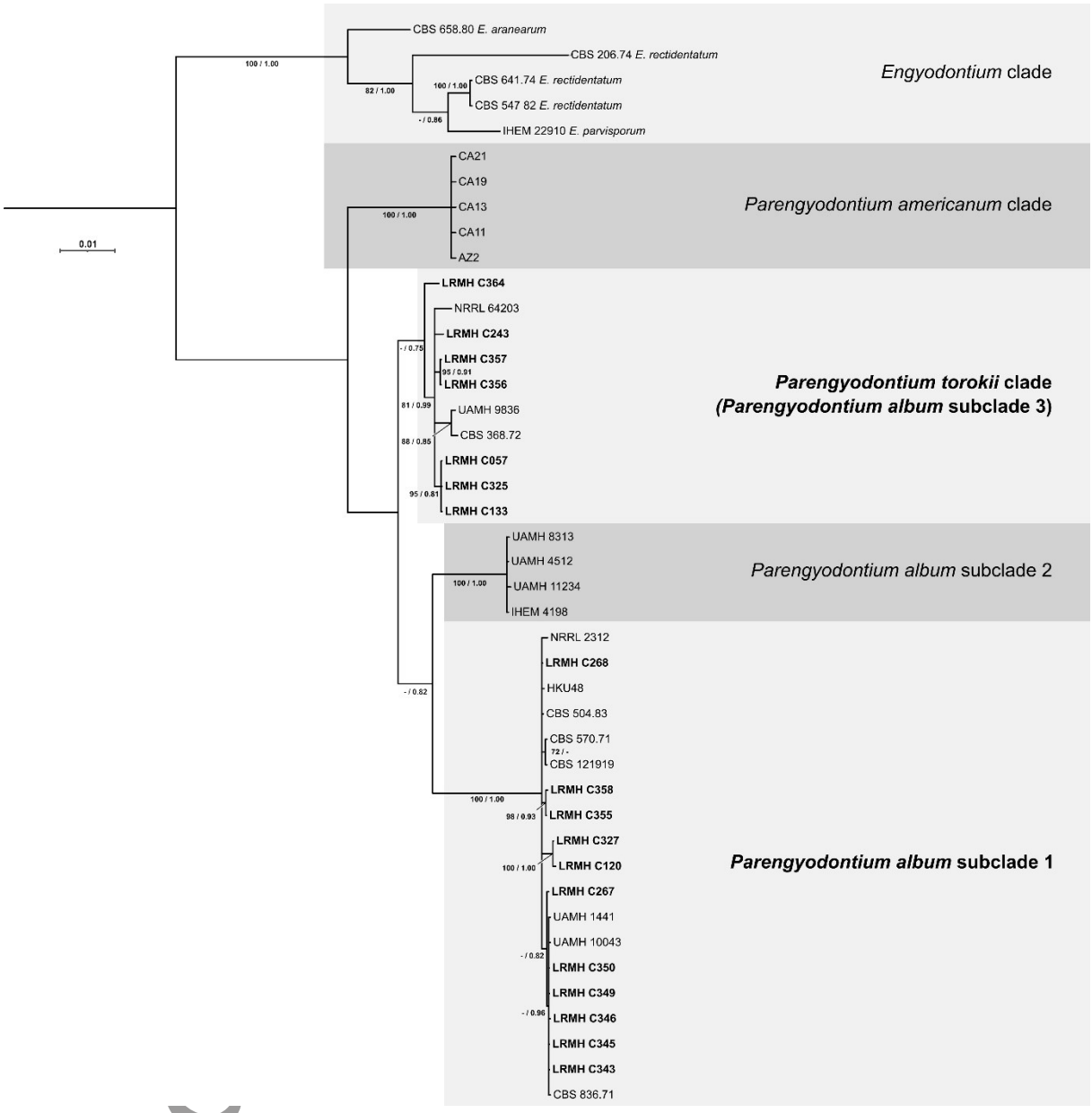

694

*corresponding author e-mail: johann.leplat@culture.gouv.fr

695 Figure 2

696

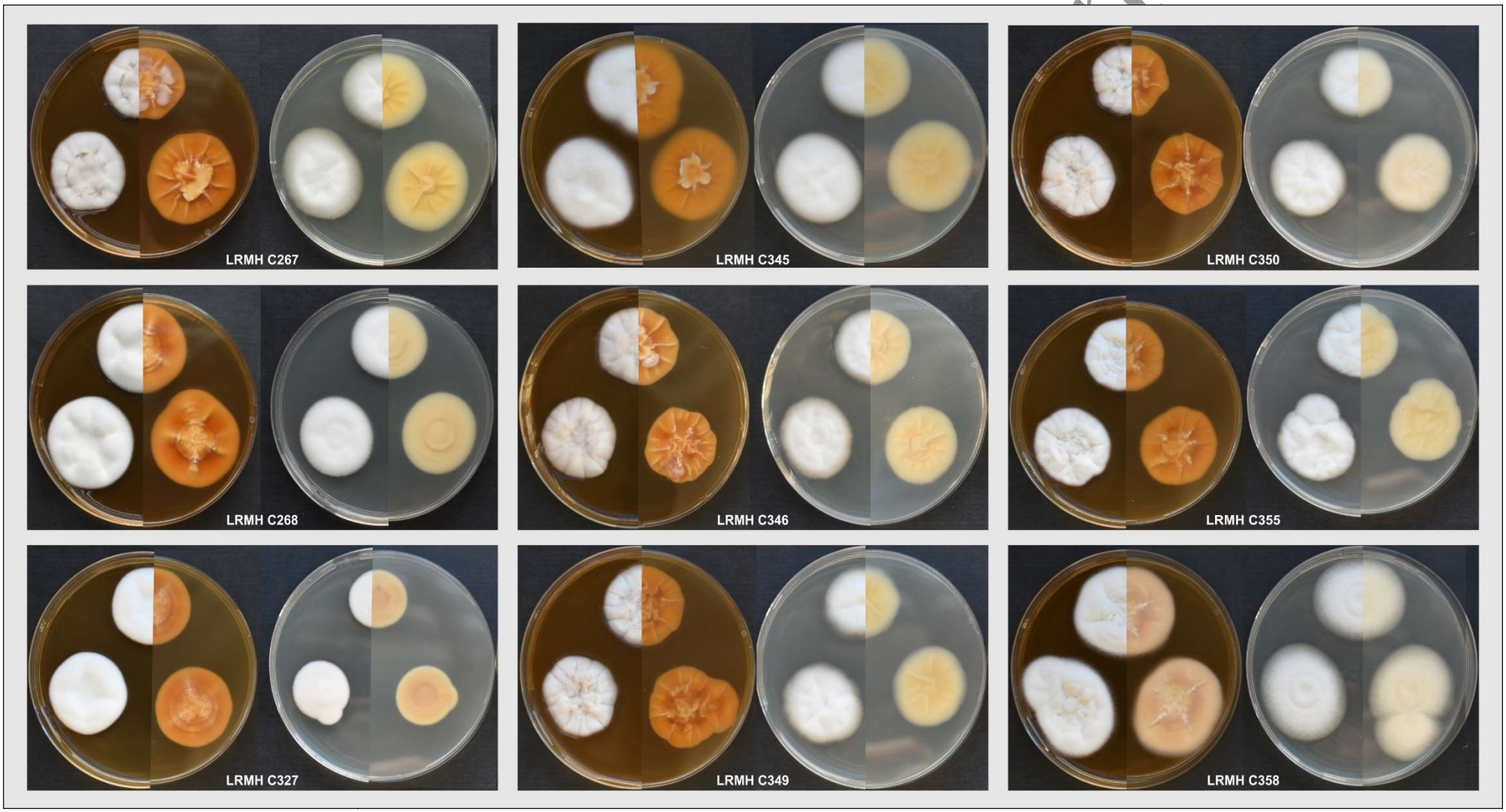

*corresponding author e-mail: johann.leplat@culture.gouv.fr

697 Figure 3

698

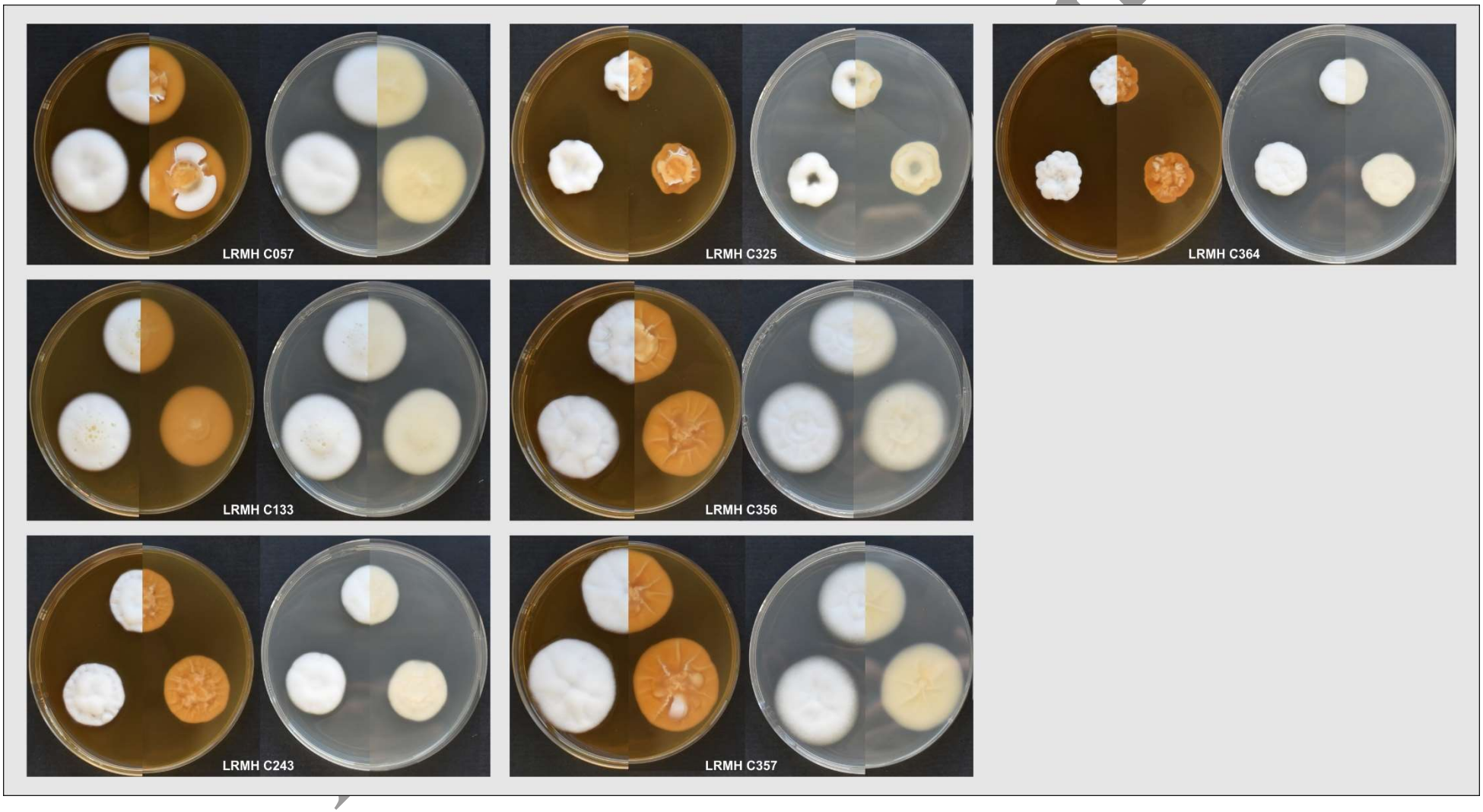

*corresponding author e-mail: johann.leplat@culture.gouv.fr

699 Figure 4

700

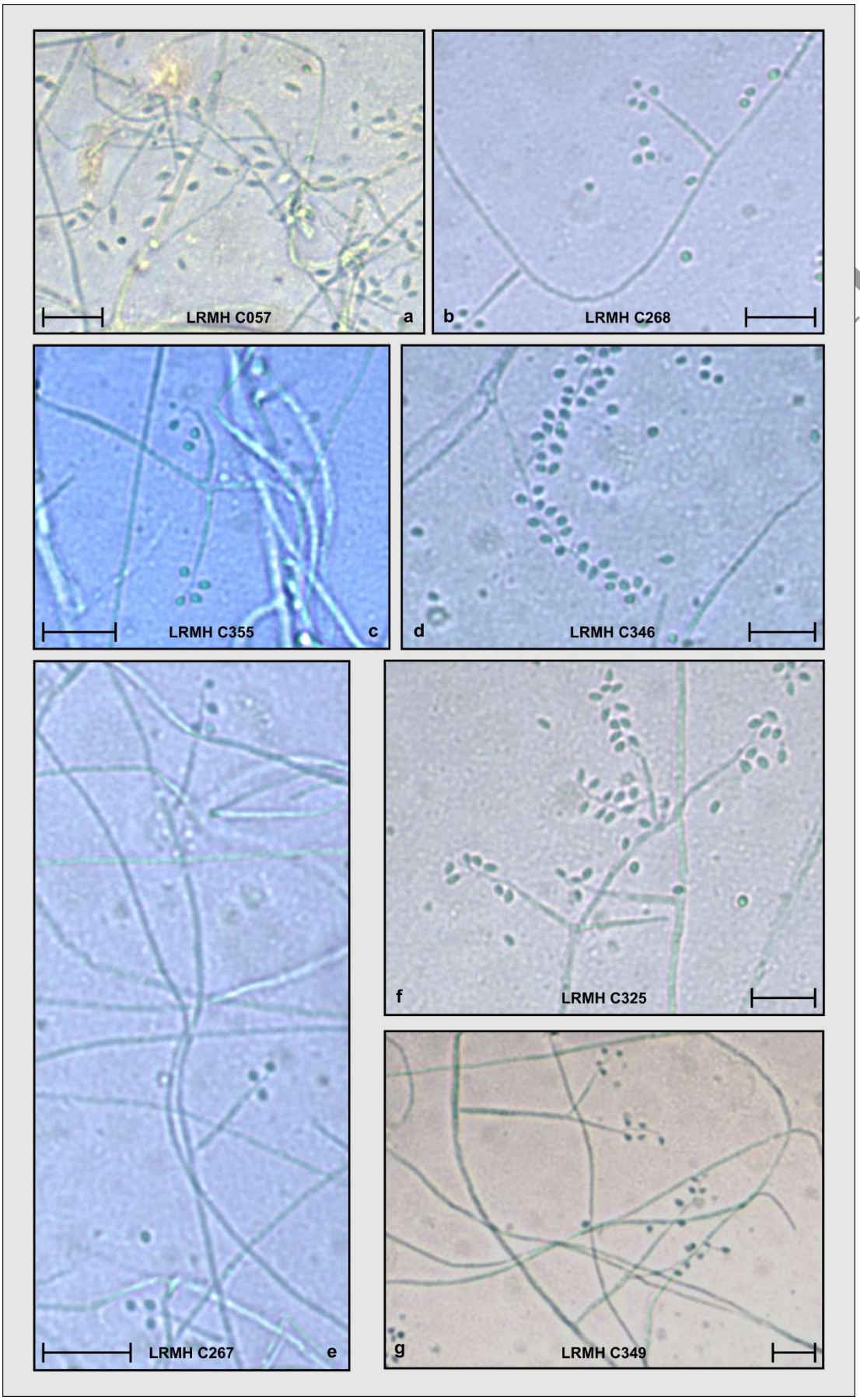

*corresponding author e-mail: johann.leplat@culture.gouv.fr

701 Figure 5

702

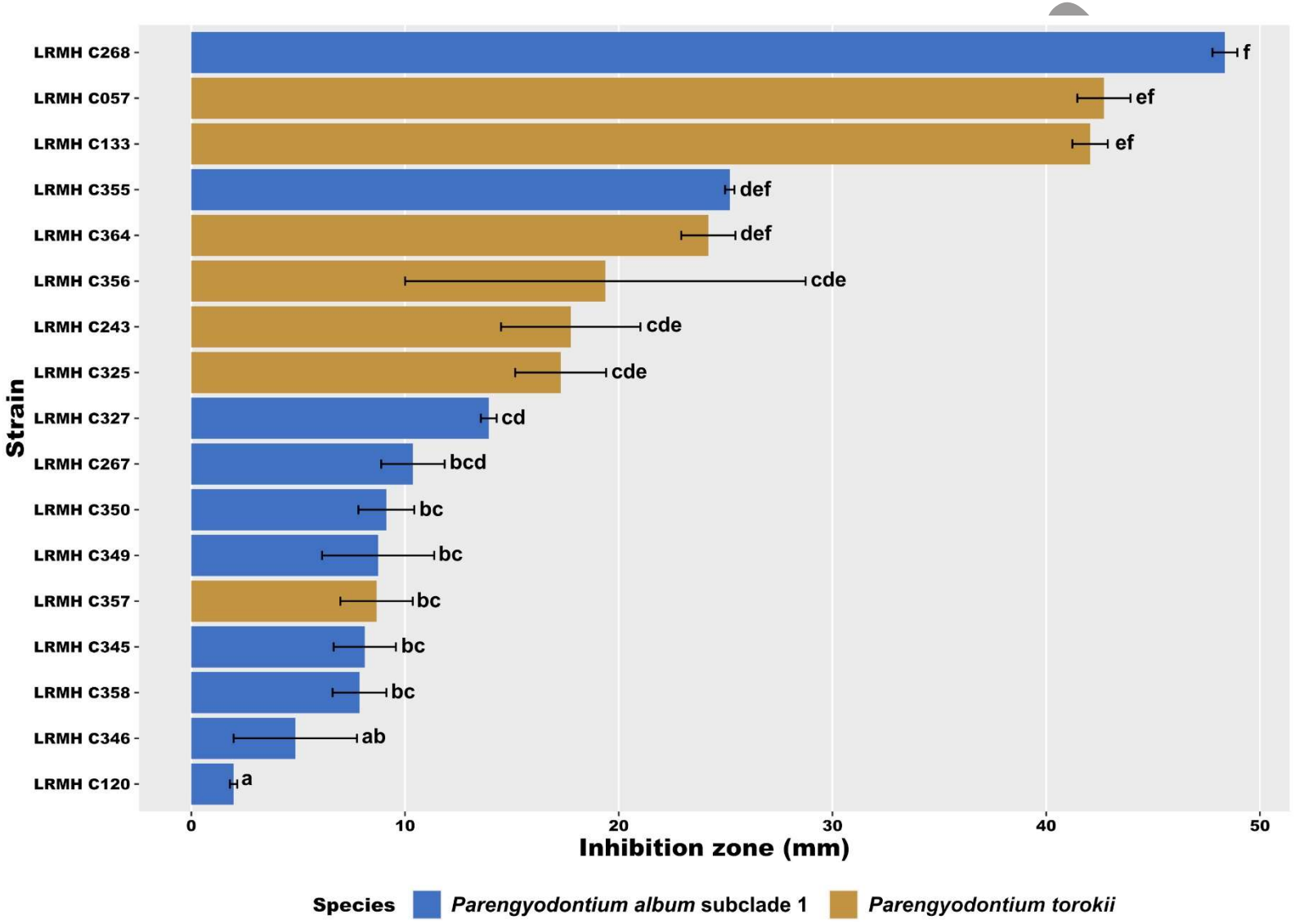

*corresponding author e-mail: johann.leplat@culture.gouv.fr